Optical and Quantum Electronics (2025) 57:85
https://doi.org/10.1007/s11082-024-08000-3

# Effects of the magnetic field, hydrostatic pressure and temperature on binding energies and optical absorption of states with donor impurity in different type quantum wells

**Esin Kasapoglu**[1]

Received: 12 November 2024 / Accepted: 17 December 2024
© The Author(s), under exclusive licence to Springer Science+Business Media, LLC, part of Springer Nature 2024

**Abstract**
In this study, the magnetic field, hydrostatic pressure and temperature dependent electronic and optical properties of asymmetric quantum wells which have some exponential potentials in the absence and presence shallow donor impurities are investigated. Calculations are made within the framework of the effective mass and parabolic band approximations. In the absence and presence of the donor impurity, we calculated the total absorption coefficient including linear and nonlinear terms for transitions between the lowest two levels. In addition, by using a variational approach, we investigated the binding energies of the 1 s and 2 s donor impurity states The results show that the total absorption peaks shift to the blue shift with the effect of external perturbations, whereas redshift in the presence of impurities. This indicates that the impurities can effectively change the band gap of semiconductors, allowing the semiconductor to absorb lower energy photons, and making it possible to design materials with special optical properties such as light absorption and emission properties.

**Keywords** Morse potential · Rosen-Morse potential · Tietz-Hua potential · Magnetic field · Hydrostatic pressure · Temperature · Binding energy

## 1 Introduction

Studies on the electronic and optical properties of low-dimensional systems have addressed the effects of different size and structure geometry, electric, magnetic and intense laser fields as well as hydrostatic pressure and temperature. One of the most important properties of low dimensional systems is that it can be doped with different types and concentrations of impurities to dramatically vary their physical, thermal, electrical, and optical properties. Thus, the impurities play a vital role in determining the impurity states in low-dimensional semiconductors and thereby can be exploited to control the optoelectronic properties of a wide range of semiconductor devices. As

✉ Esin Kasapoglu
ekasap@cumhuriyet.edu.tr

[1] Physics Department, Sivas Cumhuriyet University Science Faculty, 58140 Sivas, Turkey

known, impurities modify the band structure of semiconductor materials, the presence of impurities create the new energy levels within the bandgap, influencing the electronic and optical properties of the material. This is particularly important in the design of devices like transistors, lasers, and photodetectors. In this context, impurities can be used to tune the optical properties of semiconductor heterostructures. This is essential for applications such as light-emitting diodes (LEDs) and lasers, where precise control over the emission wavelength is required (Burgess et al. 2016; Luo et al. 2020). The binding energy plays an important role in the reliability and long-term performance of semiconductor devices. If impurities are not securely bound within the lattice, they may diffuse or migrate over time, leading to changes in device characteristics. Controlling the impurity binding energy is therefore crucial for ensuring the stability and durability of semiconductor devices. As a result, the intentional introduction of impurities and the control of impurity binding energy in semiconductor heterostructures are key aspects of semiconductor device design and fabrication. These factors allow engineers to tailor the electronic, optical, and transport properties of semiconductor materials, enabling the development of high-performance and reliable electronic devices. For this reason, electron states bounded to hydrogenic impurities and the binding energies have been extensively investigated for different semiconductor heterostructures in order to understand their dependence on the external fields, material and geometry parameters (Dakhlaoui et al. 2023a, b; Rezaei and Doostimotlagh 2012; Kasapoglu et al. 2004, 2008; Fakkahi et al. 2021; Datta et al. 2023; Hu et al. 2018; Kasapoglu 2008, 2009; Lima et al. 2007; Sadeghi and Naghdi 2014; En-nadir et al. 2023). In this study, we investigated the effects of the magnetic field, hydrostatic pressure and temperature on the electronic and optical properties of asymmetric quantum wells (QWs) with some exponential potentials such as standard Morse, improved Rosen-Morse and Tietz-Hua in the absence and presence of donor impurities.

## 2 Theory

In the effective mass approximation, The QW Hamiltonian as a function of the hydrostatic pressure and the temperature in the presence of a magnetic field is given by

$$H = \frac{1}{2m^*(P,T)}\left[\vec{p} + \frac{e}{c}\vec{A}(\vec{r})\right]^2 + V(z,P,T) - \frac{e^2}{\varepsilon(P,T)r} \tag{1}$$

where $\vec{p}$ is the momentum of the electron, $\vec{A}(\vec{r})$ is the vector potential of the magnetic field, magnetic field is applied perpendicular to the growth direction (z-direction), i. e., magnetic field and vector potential have the forms of $\vec{B} = (B, 0, 0)$ and $\vec{A} = (0, Bz, 0)$, $e$ is the elementary charge, c is the speed of light.

$m^*(P,T)$ and $\varepsilon\,(P,T)$ are the hydrostatic pressure and temperature dependent effective mass of electron and static dielectric constant, $r = \sqrt{\rho^2 + (z - z_i)^2}$ is the distance between the electron and donor impurity in the (x–y) plane ($\rho = \sqrt{x^2 + y^2}$), $z$ and $z_i$ are the coordinates of electron and donor impurity, respectively.

The hydrostatic pressure and temperature dependent effective mass for the electron is given by Sali and Satori (2014), El-Bakkari et al. (2018) and Ehrenreich (1961)

$$m^*(P,T) = \frac{m_0}{1 + E_p^{\Gamma}\left[\frac{2}{E_g^{\Gamma}(P,T)} + \frac{1}{E_g^{\Gamma}(P,T)+\Delta_0}\right]} \tag{2}$$

where $m_0$ is the free electron mass, $E_p^{\Gamma} = 7.51\text{eV}$ is energy related to the momentum matrix element for T = 0, $\Delta_0 = 0.341\text{eV}$ is spin–orbit splitting and $E_g^{\Gamma}(P,T)$ is the hydrostatic pressure and temperature dependent energy gap for the GaAs quantum well at the Γ-point in the units of eV. It is given by Kasapoglu et al. (2008); Welber et al. 1975)

$$E_g^{\Gamma}(P,T) = E_g^{\Gamma}(0,T) + 1.26\times10^{-2}P - 3.77\times10^{-5}P^2 \tag{3}$$

where $E_g^{\Gamma}(0,T) = 1.519 - \left(5.405\times10^{-4}T^2\right)/(T+204)\text{eV}$.

The hydrostatic pressure in the unit of kbar and the temperature in the unit of Kelvin (K) dependent static dielectric constant is given by Kasapoglu et al. (2008); Welber et al. 1975)

$$\varepsilon(P,T) = \begin{cases} (i)12.74e^{-1.73\times10^{-3}P}e^{9.4\times10^{-5}(T-75.6)}; \text{for } T < 200\text{K}, \\ (ii)13.18e^{-1.73\times10^{-3}P}e^{20.4\times10^{-5}(T-300)}; \text{for } T \geq 200\text{K}, \end{cases} \tag{4}$$

where the charge image effects have not been considered (i.e. $\varepsilon_w(P,T) = \varepsilon_b(P,T)$). In the presence of the shallow donor impurities, the energies of the 1 s and 2 s states are calculated through a variational approach. For each state, the trial wavefunction-$\psi(\rho,\varphi,z,\lambda)$ is as follows

$$\psi(r,\varphi,z,\lambda) = \phi(z)\,\chi(r,\varphi,z,\lambda), \tag{5}$$

where $\phi(z)$ and $\chi(r,\varphi,z,\lambda)$ are the envelope wavefunctions and hydrogenic wave functions.

The hydrogenic type wavefunctions for 1 s and 2 s states are given by Ed-Dahmouny et al. (2022)

$$\chi_{1s}\left(r,z,\lambda_{1s}\right) = N_1 exp\left(-\frac{\sqrt{\rho^2+(z-z_i)^2}}{\lambda_{1s}}\right) \tag{6}$$

$$\chi_{2s}\left(r,z,\lambda_{1s}\right) = N_2\left(2 - \frac{\sqrt{\rho^2+\left(z-z_i\right)^2}}{\lambda_{2s}}\right)exp\left(-\frac{\sqrt{\rho^2+\left(z-z_i\right)^2}}{2\lambda_{2s}}\right), \tag{7}$$

respectively. Where $N_1$ and $N_2$ are the normalization constants, $\lambda_{1s}$ and $\lambda_{2s}$ are the variational parameters.

The binding energy of the ground and first excited impurity states is given by

$$E_b = E_z - \underset{\lambda_{1s,2s}}{min}\langle\psi|H|\psi\rangle \tag{8}$$

where, $E_z$ is the ground-state energy of electron in the QW and second term gives the impurity energies $E_{1s}$ and $E_{2s}$ which are found by minimizing the expectation value of the Hamiltonian in Eq. (1) with respect to $\lambda_{1s}$ and $\lambda_{2s}$, respectively. To solve the Schrödinger equation for Hamiltonian in the Eq. (1) which means to find $\varphi(z)$ and $E_z$, is used the diagonalization method by choosing orthonormal base functions that are solutions of an infinite

square quantum well with $L$-width. $L$ is at the far end of the QW which is large enough when compared with the QW widths considered, and its value is determined according to the convergence of the energy eigenvalues. When calculating the wave function$\varphi(z)$, we ensured that the $E_z$ eigenvalues are independent of the chosen infinite potential well width-$L$, and the wave functions are localized in the well region. This method requires embedding any well potential into an infinite square well, whose presence of the confining walls does not affect the solutions. The method used for calculating the wave functions and energy levels has been previously used in many studies and the accuracy degree is quite sufficient, see for instance (Kasapoglu et al. 2019; Duque et al. 2011).

$V(z,P,T)$ is the QW potential that confines the electron. Functional expressions of the potentials as a function of position, pressure and temperature we used in this study are given as below,

$$V_M(z,P,T) = V_0(P,T)\left(1 + e^{-2z/k(p)} - 2e^{-z/k(p)}\right) \tag{9}$$

$$V_{IRM}(z,P,T) = V_0(P,T)\left(1 - \frac{e^{z_o/k(P)} + 1}{e^{z/k(P)} + 1}\right)^2 \tag{10}$$

$$V_{TH}(z,P,T) = V_0(P,T)\left(\frac{1 - e^{z/k(P)}}{1 - \kappa\, e^{z/k(P)}}\right)^2 \tag{11}$$

and are called standard Morse, improved Rosen-Morse (IRM), and Tietz-Hua (TH) potential functions, respectively. where $z_o$ is the minimum point of the potential, it shows also the distance from the equilibrium position, $V_o(P,T)$ is the temperature and hydrostatic pressure dependent finite barrier height, $k(P)$ is the hydrostatic pressure dependent width parameter ($k$ and $\kappa$ are the structure parameters that control the well width and the potential depth), and its pressure dependence is given given by Welber et al. (1975) and Mora-Ramos et al. (2012)

$$k(P) = k_0(1 - \left(S_{11} + 2S_{12}\right)P) \tag{12}$$

where $k_0$ is the value in the zero hydrostatic pressure, $S_{11} = 1.16 \times 10^{-3}\text{kbar}^{-1}$ and $S_{12} = -3.7 \times 10^{-4}\text{kbar}^{-1}$ are the elastic for GaAs material. The barrier height is given by Restrepo et al. (2013)

$$V_0(P,T) = Q_c \Delta E_g^{\Gamma}(x,P,T) \tag{13}$$

where $Q_c(= 0.6)$ is the conduction band offset parameter, $x_{Al}$ is the mole fraction of aluminum in $Ga_{1-x}Al_xAs$ layer ($x_{Al} = 0.3$), and $\Delta E_g^{\Gamma}(x,P)$ is the hydrostatic pressure dependent band gap difference between quantum well and the barrier matrix at the $\Gamma$-point. It is given by

$$\Delta E_g^{\Gamma}\left(x_{Al},P\right) = \Delta E_g^{\Gamma}\left(x_{Al}\right) - 1.3 \times 10^{-3}P, \tag{14}$$

where

$$\Delta E_g^{\Gamma}\left(x_{Al}\right) = 1.155x_{Al} + 0.37x_{Al}^2 \tag{15}$$

$\Delta E_g^{\Gamma}\left(x_{Al}\right)$ is the variation of the energy gap difference.

After obtaining the eigenvalues and eigenfunctions from the solution of Eq. (1), linear, third order nonlinear and total absorption coefficients (TAC) are found for transitions between any two electronic states by using the perturbation expansion and the density matrix methods (Dakhlaoui et al. 2023a, 2023b; Kasapoglu 2008; Kopf et al. 1992; Baskoutas et al. 2011; Keshavarz and Karimi 2010; Karabulut et al. 2011; You et al. 2021; Zhao et al. 2020), respectively

$$\beta^{(1)}(\omega)=\sqrt{\frac{\mu_o}{\varepsilon_r}}\frac{\left|M_{ij}\right|^2\sigma_v\hbar\omega\Gamma_{ij}}{(E_{ij}-\hbar\omega)^2+(\hbar\Gamma_{ij})^2}, \tag{16}$$

$$\beta^{(3)}(\omega,I)=-2\sqrt{\frac{\mu_o}{\varepsilon_r}}\left(\frac{I}{\varepsilon_o n_r c}\right)\frac{\left|M_{ij}\right|^4\sigma_v\hbar\omega\Gamma_{ij}}{\left[(E_{ij}-\hbar\omega)^2+(\hbar\Gamma_{ij})^2\right]^2}$$
$$\left(1-\frac{\left|M_{jj}-M_{ii}\right|^2}{\left|2M_{ij}\right|^2}\frac{(E_{ij}-\hbar\omega)^2-(\hbar\Gamma_{ij})^2+2E_{ij}(E_{ij}-\hbar\omega)}{E_{ij}^2+(\hbar\Gamma_{ij})^2}\right), \tag{17}$$

$$\beta(\omega,I)=\beta^{(1)}(\omega)+\beta^{(3)}(\omega,I), \tag{18}$$

where, $\varepsilon_r=n_r^2\varepsilon_0$ is the real part of the permittivity, $n_r=\sqrt{\varepsilon}$ (depending on the temperature value, and $\varepsilon$-value in (i) or (ii) of Eq. (4) is used), $\sigma_V$ is the carrier density in the system, $\mu_o$ is the vacuum permeability, in the absence donor impurity $E_{ij}=E_j-E_i$ is the energy difference between two energy levels of the electron (in the presence of donor impurity, it is defined as $E_{12}=E_{2s}-E_{1s}$ or $E_{12}=E_b^{2s}-E_b^{1s}$), $M_{ij}=\left|\langle\psi_i\left|ez\right|\psi_j\rangle\right|,(i,j=1,2)$ is the transition matrix element between the eigenstates $\psi_i$ and $\psi_j$ for incident radiation polarized in the z-direction, $\Gamma_{ij}(=1/T_{ij})$ is the relaxation rate, $T_{ij}$ is relaxation time of the interlevel transition, $c$ is the speed of the light in free space, and $I$ is the intensity of incident photon with the $\omega$-angular frequency that leads to the intersubband optical transitions.

## 3 Results and Discussions

The parameter values in our numerical calculations are $\varepsilon_o=8.85x10^{-12}\mathrm{C^2N^{-1}m^{-2}}$, $T_{12}=0.4\,ps$,$\Gamma_{12}=1/T_{12}$, $\mu_o=4\pi\,x10^{-7}\mathrm{Hm^{-1}}$, $\sigma_v=3.0x10^{22}$ e/m$^3$ and $I=5.0x10^8\,W/m^2$. These parameters are suitable for GaAs/ GaAlAs hetero-structures (Maleki et al. 2023).

For $B=0$ and $B=15T$ values of the magnetic field, potential profiles of the standard Morse, IRM, and TH QWs and the squared wave functions of the ground state electron confined in the specified wells as a function of the z-coordinate are given in Fig. 1a–c, respectively. When the $\kappa$-parameter approaches to zero, the TH QW turns into the standard Morse QW. It should be noted that the results obtained in this study are only for $k_o=20$nm (in the case of $=0$ $k=20nm$) and $\kappa=0.05$. In Fig. 1b, if the parameter-$z_o$ equals to zero, the structure has a symmetrical character, if not zero, it becomes asymmetrical character. It should be noted that, in this study it is preferred the asymmetric structure because in the symmetric case since the two s-like states considered in the transition states have even

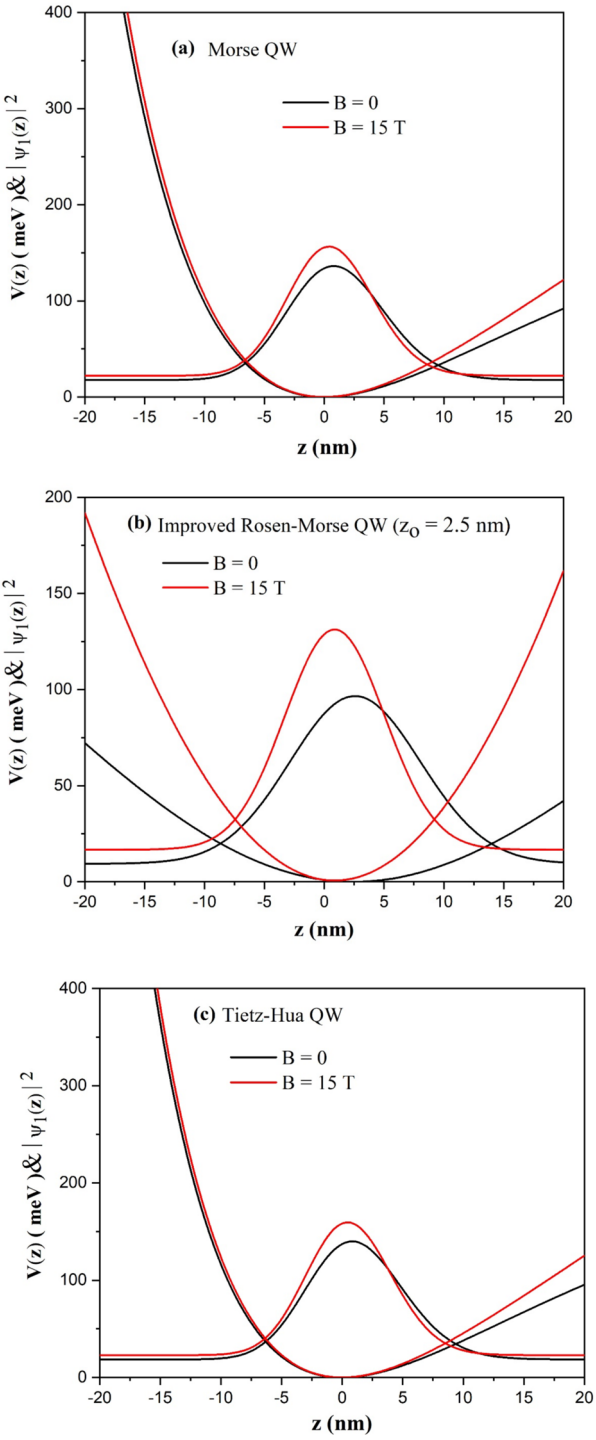



**Fig. 1** For $k = 20nm$ (in the absence of the pressure, $k$ is equal to $k_o$), quantum well profiles with the exponential type confinement potential, and squared wave functions corresponding to the ground state of the electron localized within the well as a function of the $z$-growth direction coordinate: standart Morse QW (**a**), Improved Rosen-Morse QW for $z_o = 2.5$nm (**b**), and Tietz-Hua QW (**c**). Black lines (red lines) are for $B = 0(B = 15T)$. The energy axis value of the wave functions shows the energy of the relevant level

symmetry the dipole matrix elements would be zero and also the transition would not be observed.

The variations of total absorption coefficients for a transition that is called the (1–2) transition between the ground and first excited states of an electron confined in the quantum well as a function of the incident photon energy according to some values of magnetic field, hydrostatic pressure, and temperature are given in Fig. 2a–c for the Morse QW, IRMQW, and THQW, respectively. Due to the strong confinement created by the magnetic field, the energies of the first two lowest levels of the electron and the energy difference between these levels increase, and so the absorption peaks shift towards higher photon energies with increasing amplitudes for all three QW profiles we examined. As the hydrostatic pressure increases, the dielectric constant and well width decrease, while the energies considered, the energy difference between these levels, and the effective mass of the electron increase. For this reason, a blue shift is observed in the peak positions according to the peak positions observed in the absence of magnetic field, hydrostatic pressure and temperature. But this shift is less than that in the magnetic field. In addition to the effects of pressure, as the temperature increases, the redshift not noteworthy in the peak positions is observed due to the slight decrease in the energy difference between the energy levels of interest. As seen at the insets of Figs. 2a and c, amplitudes and positions of the absorption peaks for QWs in Fig. 1a and c become very close due to the decreasing $\kappa$-value. Finally, for $\kappa = 0$, the results for both structures overlap completely.

When the absorption peaks belong to the QW profile in Fig. 1b are compared with those of the other structures, it is seen that the peak amplitudes are smaller and the peak positions are located at lower photon energies. As known, the bleaching effect occurs if the light intensity that provides optical transitions is very strong, and two energy levels of interest for the transition are close to each other. It is observed that the bleaching effect disappears when lower light intensity than here is used, apart from changing the structure parameters and/or applying external fields (Maleki et al. 2023). With the effect of the strong confinement created by the magnetic field, the bleaching effects observed in the absence of the magnetic field disappear. And indeed, while this effect in Figs. 2a and c disappears thanks to external perturbations, it is observed to decrease significantly in Fig. 2b. Due to the strong confinement created by the magnetic field, the energies of the first two lowest levels of the electron and the energy difference between these levels increase for all QWs.

To better see the differences between Fig. 2a, c and b, the variations of total absorption coefficients for the (1–2) transition of the electron confined in all QW types considered for three different hydrostatic pressure values as independent from temperature and magnetic field as a function of the incident photon energy are given in Fig. 3. As the pressure increases, the absorption peaks shift to blue with increasing amplitudes, the peaks belonging to the IRM QW with respect to the other QWs are located at lower photon energies and they have smaller amplitudes. When the peaks belonging to the other two wells are compared, it is observed that although the peaks are very close to each other, the peaks belonging to the TH QW have larger amplitudes and are located at higher photon energies.

The binding energies of 1 s and 2 s impurity states versus the impurity position-$z_i$ for different magnetic field, hydrostatic pressure and temperature values are given in Fig. 4a–c for the standard Morse QW, IRM QW, and TH QW, respectively. Solid and dashed lines correspond to the binding energies of 1 s and 2 s impurity states. The binding energy for the 1 s impurity state is always greater than that of 2 s or the other excited impurity states because the Coulomb interaction between the electron and 1 s- donor impurity level is the strongest compared to the others (Kasapoglu et al. 2023; Kasapoglu et al. 2016). For impurities located where the probability of finding an electron is maximum (minimum)

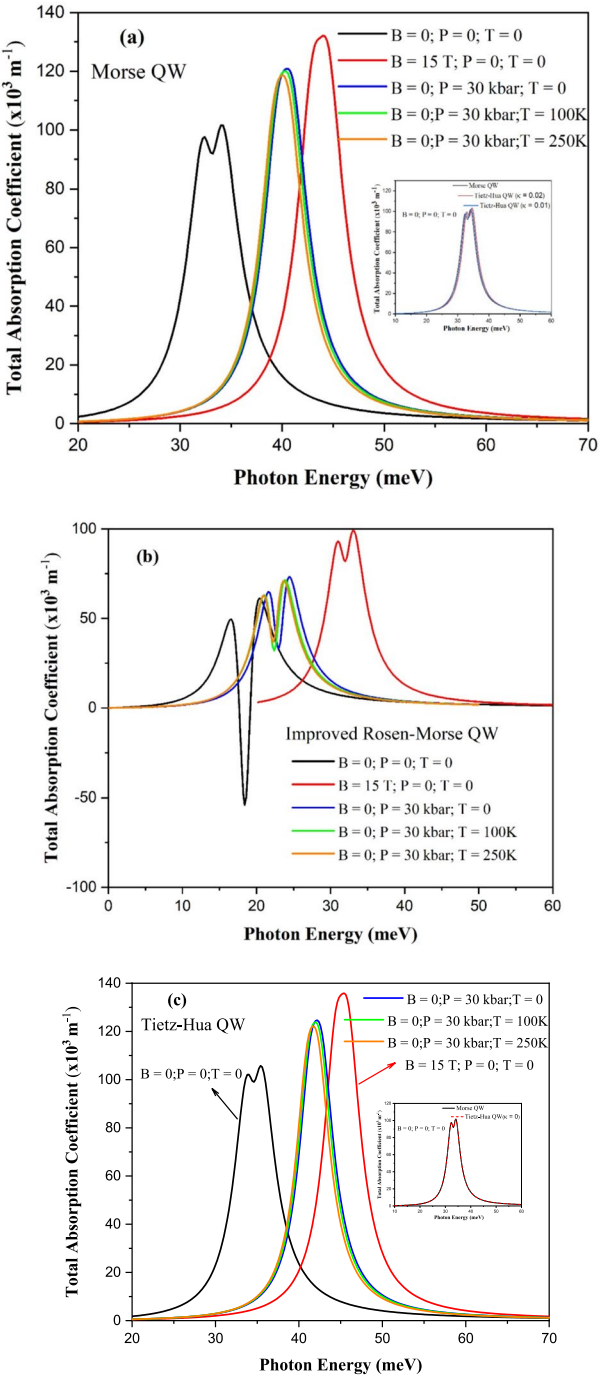



**Fig. 2** For $k_o = 20$nm, the variation of total absorption coefficients for a transition that is called the (1–2) between the ground and first excited states of an electron confined in the quantum well as a function of the incident photon energy according to the magnetic field, hydrostatic pressure and temperature values: Morse QW (**a**), Improved Rosen-Morse QW (**b**), and Tietz-Hua QW (**c**). Insets at the figure **a** and **c** shows total absorption coefficients corresponding to the Morse and Tietz-Hua QWs for $\kappa \neq 0$ and $\kappa = 0$ without magnetic field, pressure and temperature

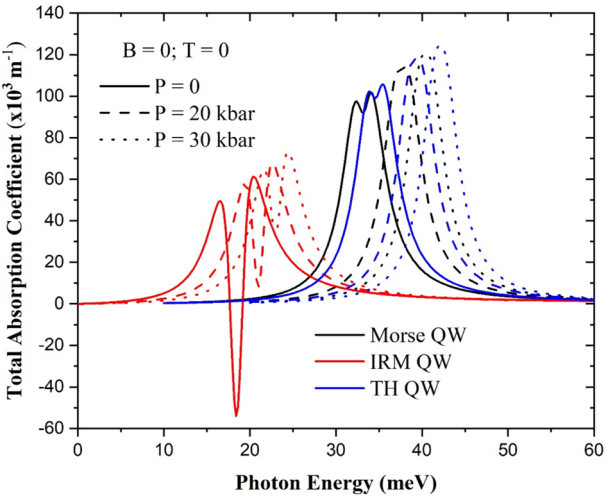



**Fig. 3** For $k_o$ = 20nm, the variations of total absorption coefficients for the (1–2) transition of the electron confined in all quantum well types considered as a function of the incident photon energy for different hydrostatic pressure values as independent from temperature and magnetic field

the binding energy becomes maximum (minimum), because the variation of the binding energy versus the impurity position completely overlaps the spatial distribution of the wave function of the electron confined in the quantum structure. Where the external perturbations taken into account make the electron more energetic and cause it to be spatially confined in a narrower region, resulting in an increase in the Columbic interaction between the electron and the donor impurity and an increase in the binding energies of each impurity state of interest. As clearly observed from the magnetic field results, this undoubtedly leads to a shift of the binding energy maximum.

In the presence of donor impurity, the effects of external perturbations are as follows: (i) Due to the magnetic field causes additional confinement, energy of electron increases, while the left side of the QWs considered becomes sharper and also rises to infinity, and results in the minimum points of these wells also shift towards zero. (ii) As the hydrostatic pressure increases, the decrease in the dielectric constant and well width, as well as the increase in the effective mass of the electron, leads to a stronger confinement within the QW of the electron, and the binding energy increases because this increases the finding probability that the electron and the donor impurity are in the same plane. The increase in donor binding energy due to hydrostatic pressure is higher than the increase due to the magnetic field. (iii) With the effect of temperature, the geometric limitation weakens at the same rate due to the slight increase in the width parameter-$k$. As the spatial spread of the electron increases, the binding energy also decreases in an insignificantly as the probability of being found near the impurity decreases.

To better analyze the behavior of the absorption peaks, the transition energies between the two lowest s-like impurity states versus the impurity position for different magnetic field, hydrostatic pressure and temperature values are given in Fig. 5a–c for Morse QW, IRM QW, and TH QW, respectively. As can be seen from these figures, the change of transition energies against the impurity position is the same as the change of impurity binding energy against the impurity position under the external perturbations considered. As mentioned above, the impurity binding energy is determined by the degree of probability of finding the electron and the impurity in the same plane. If the impurity is placed at the position where the electron probability density of the subband state becomes maximum,

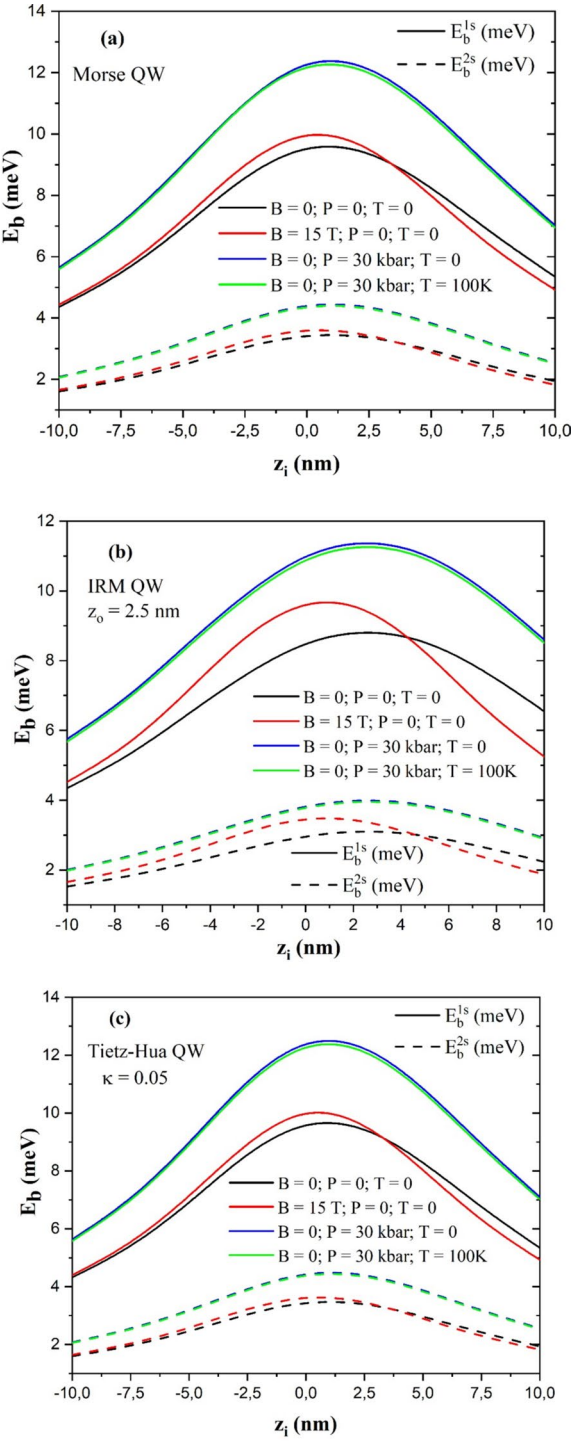



**Fig. 4** The binding energies of 1 s and 2 s impurity states versus the impurity position-$z_i$ for different magnetic field, hydrostatic pressure and temperature values: Morse QW (**a**), Improved Rosen-Morse QW (**b**), and Tietz-Hua QW (**c**). Solid and dashed lines correspond to the binding energies of 1 s and 2 s impurity states

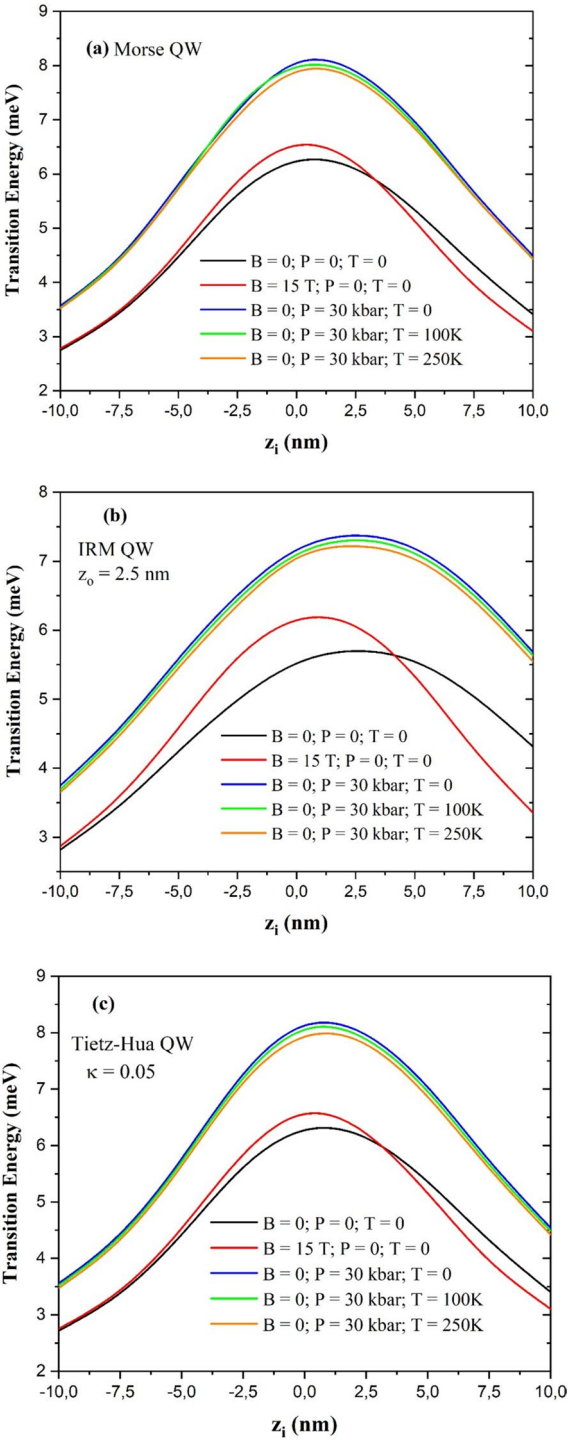



**Fig. 5** The transition energy between the first two impurity states versus the impurity position for different magnetic field, hydrostatic pressure and temperature values in Morse QW (**a**), Improved Rosen-Morse QW (**b**), and Tietz-Hua QW (**c**)

there will be a strong coupling between the impurity and the subband state. Thus one would obtained an increment in the binding energy. Therefore, where the binding energy is large, the transition energy will also be large or vice versa as seen from the equation $E_{12} = E_{2s} - E_{1s}$ or $E_{12} = E_b^{2s} - E_b^{1s}$.

The variation of the TAC for the (1 s-2 s) transition between the first two impurity states versus the incident photon energy with respect to the magnetic field, hydrostatic pressure and temperature values are given in Fig. 6a–c for the Morse QW, IRM QW, and TH QW, respectively. Where, only for $z_i = 0$ donor position, the TAC corresponding to the 1 s-2 s transition is given. The peak position of the TAC shifts towards the blue with decreasing magnitudes due to the increase in the transition energy compared to the peak positions independent magnetic field, pressure, and temperature. As can be seen from the figures given for the (1 s-2 s) transition energies, the peak positions of TAC will shift to lower photon energies for off-center donor impurity positions. Under the influence of the magnetic field, the absorption peaks have very low amplitudes due to the very small values of the dipole matrix elements and peaks shift to the lower photon energies with respect to the peaks dependent pressure and temperature. In the presence of impurities, it is observed the redshift in the absorption peak positions. This indicates that the presence of impurities can effectively change the band gap of semiconductors, allowing the semiconductor to absorb lower energy photons, and making it possible to design materials with special optical properties such as light absorption and emission properties. Tuning the bandgap is essential for applications such as photodetectors, solar cells, light-emitting diodes (LEDs), and laser diodes.

## 4 Conclusion

In this study, the binding energies of the 1 s and 2 s donor impurity states by using a variational approach, in the absence and presence of the donor impurity, the total absorption coefficient including linear and third-order nonlinear terms for transitions between lowest two electron levels are investigated for different QW profiles under the effects of the magnetic field, hydrostatic pressure and temperature. Dependence of binding energy on impurity position has the same behaviour with the spatial distribution of the wave function of the electron confined in the QW. Therefore, the binding energy becomes maximum (minimum) for impurities located where the probability of finding an electron within the QW is maximum (minimum). Magnetic field and hydrostatic pressure cause electron to be spatially confined in a narrower region, resulting in an increase in the Columbic interaction between the electron and the donor impurity and an increase in the binding energies of each impurity state of interest. The results show that depending on the magnetic field, pressure, and temperature, the total absorption peaks shift towards blue in the absence of impurities and shift towards red in the presence of impurities. These results show that impurities can effectively change the band gap of the semiconductors, allowing the semiconductor to absorb lower energy photons and making it possible to design materials with special optical properties, such as light absorption and emission properties.

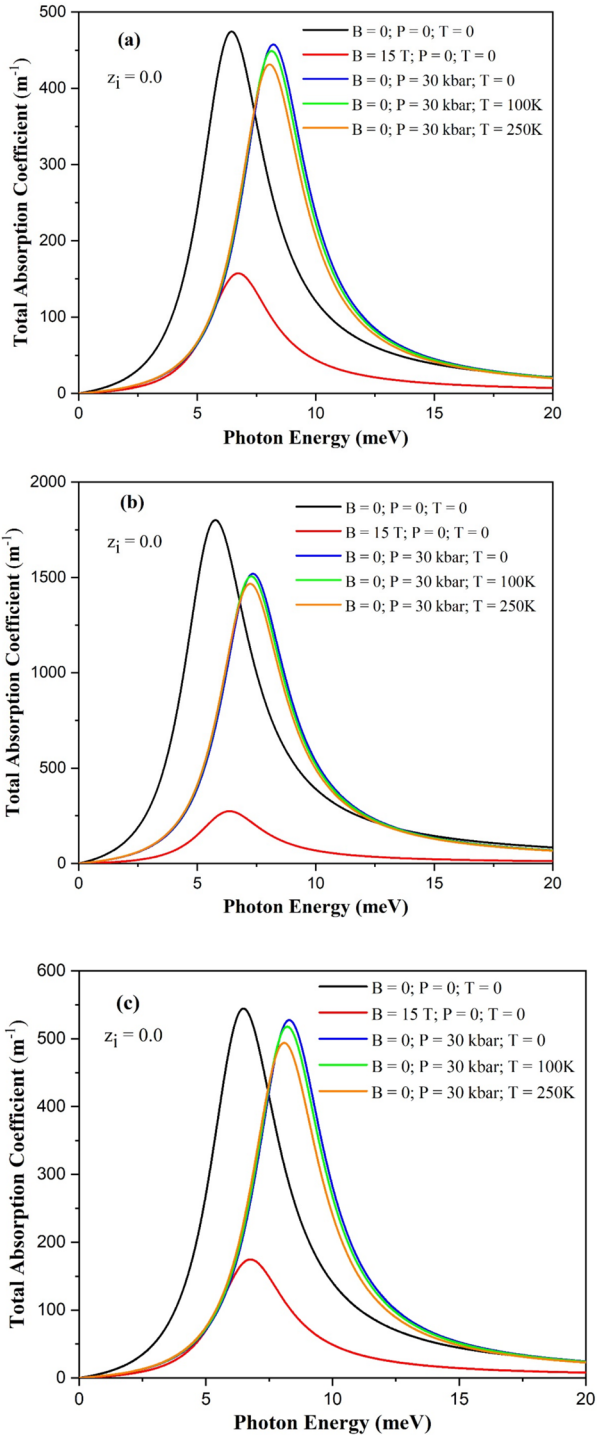



**Fig. 6** The variation of the total absorption coefficient for the (1 s–2 s) transition between the first two impurity states for on-center donor impurity versus the incident photon energy with respect to the magnetic field, hydrostatic pressure and temperature values in Morse QW (**a**), Improved Rosen-Morse QW (**b**), and Tietz-Hua QW (**c**)

**Author contributions** I am the sole author of this manuscript.

**Funding** No funding was received to conduct this study.

**Data availability** Data will be made available on request.

## Declarations

**Conflict of interest** The authors declare no competing interests.

## References

Baskoutas, S., Garoufalis, C., Terzis, A.F.: Linear and nonlinear optical absorption coefficients in inverse parabolic quantum wells under static external electric field. Eur. Phys. J. b. **84**, 241–247 (2011)

Burgess, T., Saxena, D., Mokkapati, S., Li, Z., Hall, R.C., Davis, J.A., Wang, Y., Smith, L.M., Fu, L., Caroff, P., Tan, H.H., Jagadish, C.: Doping-enhanced radiative efficiency enables lasing in unpassivated GaAs nanowires. Nat. Commun. **7**, 11927-11933 (2016)

Dakhlaoui, H., Belhadj, W., Ungan, F., Al-Shameri, N.S.: Linear and nonlinear optical properties in GaAs quantum well based on konwent-like potential: effects of impurities and structural parameters. Physica E **152**, 115760-115773 (2023a)

Dakhlaoui, H., Belhadj, W., Musa, M.O., Ungan, F.: Binding energy, electronic states, and optical absorption in a staircase-like spherical quantum dot with hydrogenic impurity. Eur. Phys. J. plus **138**, 519–530 (2023b)

Datta, S., Ghosh, M., M.: Influence of impurity binding energy on the excitation dynamics of doped GaAs quantum dot: role of noise. J. Chem. Sci. **135**, 15-24 (2023)

Duque, C.A., Mora-Ramos, M.E., Kasapoglu, E., Sari, H., Sökmen, I.: Intense laser field effect on impurity states in a semiconductor quantum well: transition from the single to double quantum well potential. Eur. Phys. J. B. **81**, 441–449 (2011)

Ed-Dahmouny, A., Sali, A., Es-Sbai, N., Arraoui, R., Duque, C.A.: The impact of hydrostatic pressure and temperature on the binding energy, linear, third-order nonlinear, and total optical absorption coefficients and refractive index changes of a hydrogenic donor impurity confined in GaAs/AlxGa1−xAs double quantum dots. Eur. Phys. J. plus **137**(7), 784-797 (2022)

Ehrenreich, H.: Band structure and transport properties of some 3–5 compounds. J. Appl. Phys. **32**, 2155–2166 (1961)

El-Bakkari, K., Sali, A., Iqraoun, E., Rezzouk, A., Es-Sbai, N., Jamil, M.O.: Effects of the temperature and pressure on the electronic and optical properties of an exciton in GaAs/$Ga_{1-x}Al_xAs$ quantum ring. Physica B **538**, 85–94 (2018)

En-nadir, R., El-ghazi, H., Tihtih, M., Zaki, S.E., Belaid, W., Maouhoubi, I., Zorkani, I.: Exploring the electronic properties of shallow donor impurities in modified ∩-shaped potential: effects of applied electric field, parabolicity, compositions, and thickness. Eur. Phys. J. B. **96**, 78-89 (2023)

Fakkahi, A., Sali, A., Jaouane, M., M., et al.: Hydrostatic pressure, temperature, and electric field effects on the hydrogenic impurity binding energy in a multilayered spherical quantum dot. Appl. Phys. A **127**, 908-917 (2021)

Hu, M., Wang, H., Gong, Q., et al.: Comparison of external electric and magnetic fields effect on binding energy of hydrogenic donor impurity in different shaped quantum wells. Eur. Phys. J. b. **91**, 19-25 (2018)

Karabulut, İ, Mora-Ramos, M.E., Duque, C.A.: Nonlinear optical rectification and optical absorption in GaAs–$Ga_{1-x}Al_xAs$ asymmetric double quantum wells: combined effects of applied electric and magnetic fields and hydrostatic pressure. J. Lumin. **131**, 1502–1509 (2011)

Kasapoglu, E.: The hydrostatic pressure and temperature effects on donor impurities in GaAs/$Ga_{1-x}Al_xAs$ double quantum well under the external fields. Phys. Lett. A **373**, 140–143 (2008)

Kasapoglu, E.: Binding energy of donor impurities in double inverse parabolic quantum well under electric field. Physica E **41**, 1222–1225 (2009)

Kasapoglu, E., Sari, H., Sökmen, I.: Effect of crossed electric and magnetic fields on donor impurity binding energy Appl. Phys. A **78**, 101–105 (2004)

Kasapoglu, E., Sari, H., Sökmen, I.: Effects of magnetıc and electric fields on the hydrogenıc impurıty in an ellıpsoıdal parabolıc quantum dot. Surf. Rev. Lett. **15**, 201–205 (2008)

Kasapoglu, E., Sakiroglu, S., Sökmen, I., Restrepo, R.L., Mora-Ramos, M.E., Duque, C.A.: The effects of the electric and intense laser field on the binding energies of donor impurity states (1s and 2p±) and optical absorption between the related states in an asymmetric parabolic quantum well. Opt. Mater. **60**, 318–323 (2016)

Kasapoglu, E., Sakiroglu, S., Sari, H., Sokmen, I., Duque, C.A.: Binding energy and optical absorption of donor impurity states in "12-6" tuned GaAs/GaAlAs double quantum well under the external fields. Physica B **554**, 72–78 (2019)

Kasapoglu, E., Yücel, M.B., Duque, C.A.: Electronic and optical properties of the exponential and hyperbolic Rosen-Morse types quantum wells under applied magnetic field. Eur. Phys. J. plus **138**, 1026-1034(2023)

Keshavarz, A., Karimi, M.J.: Linear and nonlinear intersubband optical absorption in symmetric double semi-parabolic quantum wells. Phys. Lett. A **374**, 2675–2680 (2010)

Kopf, R.F., Herman, M.H., Schnoes, M.L., Perley, A.P., Livescu, G., Ohring, M.: Band offset determination in analog graded parabolic and triangular quantum wells of GaAs/AlGaAs and GaInAs/AlInAs. J. Appl. Phys. **71**, 5004–5011 (1992)

Lima, F.M.S., Amato, M.A., Olavo, L.S.F., Nunes, O.A.C., Fonseca, A.L.A., da Silva, E.F.: Intense laser field effects on the binding energy of impurities in semiconductors. Phys. Rev. B **75**, 073201-073204 (2007)

Luo, D., Wang, L., Qiu, Y., Huang, R., Liu, B.: Emergence of impurity-doped nanocrystal light-emitting diodes. Nanomaterials **24**, 1226-1265 (2020)

Maleki, S., Haghighatzadeh, A., Attarzadeh, A.: Linear and nonlinear optical absorption coefficients and refractive index changes of GaAs/GaAsSb/GaAs V-shaped quantum wells affected by intense laser fields. Opt. Quant. Electron. **55**, 521-534 (2023)

Mora-Ramos, M.E., Duque, C.A., Kasapoglu, E., Sari, H., Sökmen, I.: Linear and nonlinear optical properties in a semiconductor quantum well under intense laser radiation: effects of applied electromagnetic fields. J. Lumin. **132**, 901–913 (2012)

Restrepo, R.L., Barseghyan, M.G., Mora-Ramos, M.E., Duque, C.A.: Effects of hydrostatic pressure on the nonlinear optical properties of a donor impurity in a GaAs quantum ring. Physica E **51**, 48–54 (2013)

Rezaei, G., Doostimotlagh, N.A.: External electric field, hydrostatic pressure and conduction band non-parabolicity effects on the binding energy and the diamagnetic susceptibility of a hydrogenic impurity quantum dot. Phys. E **44**, 833–838 (2012)

Sadeghi, E., Naghdi, E.: Effect of electric and magnetic fields on impurity binding energy in zinc-blend symmetric InGaN/GaN multiple quantum dots. Nano Convergence **1**, 25–30 (2014)

Sali, A., Satori, H.: The combined effect of pressure and temperature on the impurity binding energy in a cubic quantum dot using the FEM simulation. Superlattices Microstruct. **69**, 38–52 (2014)

Welber, B., Cardona, M., Kim, C.K., Rodriquez, S.: Dependence of the direct energy gap of GaAs on hydrostatic pressure. Phys. Rev. B **12**, 5729-5738 (1975)

You, J., Guo, K., Lao, J., Mo, S.: Linear and nonlinear optical absorption coefficients and refractive index changes of zigzag quantum wells affected by terahertz laser field. Thin Solid Films **733**, 138813-138818 (2021)

Zhao, Q., Aqiqi, S., You, J.F., Kria, M., Guo, K.X., Feddi, E., Zhang, Z.H., Yuan, J.H.: Influence of position-dependent effective mass on the nonlinear optical properties in algaas/gaas single and double triangular quantum wells. Phys. E **115**, 113707-113713 (2020)

**Publisher's Note** Springer Nature remains neutral with regard to jurisdictional claims in published maps and institutional affiliations.

Springer Nature or its licensor (e.g. a society or other partner) holds exclusive rights to this article under a publishing agreement with the author(s) or other rightsholder(s); author self-archiving of the accepted manuscript version of this article is solely governed by the terms of such publishing agreement and applicable law.